Dyes and Pigments 145 (2017) 436–443

Contents lists available at ScienceDirect

Dyes and Pigments

journal homepage: www.elsevier.com/locate/dyepig

Facile synthesis of high antistatic mica-titania@graphene composite pearlescent pigment at room temperature

Yan Wang [a, b], Ziwei Liu [a], Xiaoyu Lu [a], Guanhong Lu [a], Jing Sun [a, *]

[a] State Key Laboratory of High Performance Ceramics and Superfine Microstructures, Shanghai Institute of Ceramics, Chinese Academy of Sciences, Shanghai 200050, China
[b] University of Chinese Academy of Sciences, 19 Yuquan Road, Beijing 100049, China

ARTICLE INFO

Article history:
Received 3 May 2017
Received in revised form
14 June 2017
Accepted 15 June 2017
Available online 16 June 2017

Keywords:
Facile synthesis
Antistatic composite pearlescent pigment
Znic powder
Room temperature
Graphene

ABSTRACT

A facile and rapid method is reported to effectively in synthesizing high performance graphene based mica-titania antistatic pearlescent pigment. Znic powder is firstly introduced to prepare the composite pearlescent pigment as a reduction catalyst. Through a comparative analysis with previous Argon annealing reduction method, it can obviously increase 100–4600 fold antistatic performance of mica-titania pearlescent pigment at room temperature in a short time. The minimum volume resistivity of as-prepared composite pigments is 12 kΩ cm and decreases about 10^4 times than that without graphene. The composite pearlescent pigment samples also remain the silver white pearlescent effect, as well as that of raw mica-titania pigment. The stability of titanium chemical state and reduced graphene oxide have been proved by Raman and X-ray photoelectron spectroscopy tests. Since the method is efficient, relatively environmental friendly and low cost, it could be expected to satisfy a large-area application of antistatic pearlescent pigment.

1. Introduction

Mica-titania (MT) pearlescent pigment is a high valuable additive due to its unique color and angle-dependent optical effects, which is widely applied in the fields of electronic industry, plastics, printed products, and automobile paints for decorative purposes [1–3]. Their iridescent and analogous pearl shining color are derived from the multiple interference effect between high refractive index titania nanoparticles (TiO_2 NPs) shell and low refractive index mica core [4,5]. However, the core-shell structure of MT pigment leads to side effect, such as hidden fire hazard and electromagnetic interference dangers, due to the electric insulation of TiO_2 NPs semiconductor and mica simultaneously [6]. In the last twenty years, scientists focus on solving the static electricity aggregation problem by coating SnO_2-Sb_2O_3 (ATO) on the surface of MT pigments [7,8]. Admitting that ATO is a high-performance conductive material, relatively low refractive index and strong blue light absorbed in visible region of ATO greatly affect the original color effect of MT pigments [9,10]. Furthermore, the structural integrity of shell layer could be destroyed during the calcined procedure since the poor adhesion between ATO and MT pigment [10,11]. So the luster effect of MT pigments sharply decreases with the increase of conductivity. Thus, it urgently needs to break through the present structure and component of MT@ATO composite pearlescent pigment.

In our previous work, a novel mica-titania@reduced-graphene (MT@rGO) composite pearlescent pigment is reported to endow MT pigment with antistatic property by introducing graphene [12]. The minimum volume resistivity of MT@rGO pigments is about 14 MΩ cm and approximately one fourteenth of that of pristine MT pearlescent pigment at the same pressure after Ar annealing reduction. Meanwhile the lightness of MT@rGO pigments obviously also increases 1–5%. In view of the core-shell structure of MT@rGO composite pearlescent pigment, its antistatic property is determined by the distribution character continuity and reduction degree of rGO [13]. And the reduction degree of rGO strongly depends on the reductant and reduction method [14]. Although MT@rGO antistatic composite pearlescent pigment with high lightness could be obtained through the high temperature gas phase reduction due to TiO_2 crystallization, it inevitably causes the loss of graphene nanosheets which leads to a decrease of antistatic ability of composite pigment [15]. What's worse, several hundred calcined temperature using in the reduction procedure also extremely limits its

* Corresponding author.
E-mail address: jingsun@mail.sic.ac.cn (J. Sun).

http://dx.doi.org/10.1016/j.dyepig.2017.06.042
0143-7208/

large-scale application when considering issues of the expensive equipment, long heating time and uniformity.

Among the numerous graphene reduction methods, the metal acid reduction method has been studied extensively for its instantaneous reduction time [16–19]. The common reductant could be transition metals, such as Zn, Fe, Mg and so on. Znic powder was firstly reported to reduce GO in 2011 at room temperature by the ultrosonicated-assisted within 1 min, which residual rGO's conductivity is about 15,000 S/m [20]. The rapid and efficient reduction process is expected to maintain the interface stability between MT and graphite oxide (GO), since they have similar acid reaction solution with that of synthesis of MT@GO composite pearlescent pigments. And more important, compared with high temperature calcined reduction procedure, this liquid phase reduction method is suitable for large-scale area application due to low cost and relatively environmental friendly.

In summary, we report a facile efficient reduction method to prepare high performance MT@rGO antistatic composite pearlescent pigment by using znic powder as a reductant in a mild acidic solution at room temperature in this work. The results show that the conductivity of MT@rGO composite pearlescent pigment increases 10^4-fold than that of MT pigments. And the minimum volume resistivity of MT@rGO composite pearlescent pigment is about 12 kΩ cm, which is similar with that of reported MT@ATO pigment ranging from 10^4 to 10^6 Ω cm [11]. What's more, this method is significantly simpler, faster and more efficient, which could be an ideal procedure for industrial manufacture. In this case, the high antistatic performance of MT@graphene composite pearlescent pigment is anticipated to provide new possibilities for the application of MT pigment as the functional and decorative additive.

2. Experimental

2.1. Materials

Znic powder (D_{50} < 50 μm) was purchased from Aladdin Reagent Co., Ltd. The mica was obtained from Hangzhou Forward Fine Chemicals CO., LTD, China and its particle size distribution ranges from 10 to 60 μm. 325 mesh graphite flakes and all analytical grade chemicals were purchased from Shanghai Sinopharm Chemical Reagent Co., Ltd. (Shanghai, China) and used as received. Distilled water was used in all studies.

2.2. Synthesis of MT@graphene composite pearlescent pigments

Graphene oxide (GO) was prepared by the modified Hummers' method and dispersed in distilled water with a concentration of 20 mg/mL. A silver white mica-titania (MT) pearlescent pigment was synthesized by $TiCl_4$ hydrolysis method and dispersed in HCl solution (pH = 4.0). A certain volume GO solution was constantly added dropwise into the 5 wt% MT suspension solution with stirring. After dropping, the mixture solution was refluxed for 8 h at 100 °C. Thereafter, the MT@GO composite pearlescent pigments were obtained by filtration and vacuum drying. The samples were denoted with different added amount of GO in MT@GO composites as MT@GO-x (x = 0–4 wt%).

The MT@reduced GO (MT@rGO) composite pearlescent pigments were prepared by ultrafast reduction method based on Ouyang's work with some modifications [20]. Briefly, 1.0 g MT@GO-x (x = 0–4) composite pearlescent pigment and 0.1 g znic powder were suspended in 100 mL aqueous solution at room temperature with stirring. 1 mL HCl (35 wt%) was dropwise added into the mixture solution within 1 min under stirring and the pH value is adjusted to 4.0 ± 0.2 by 0.1 M NaOH. Then the mixture was stirring until all znic powder completely dissolved. The MT@rGO-x (x = 0–4) composite pearlescent pigments were collected after filtration, washed with distilled water several times, and vacuum drying.

2.3. Characterization

The cross-section and surface morphologies of MT@graphene composite pearlescent pigments were observed by Field Emission Scanning Electron Microscope with a Magellan 400 FEI, which the operation voltage was 10 kV. The crystalline phase identification was taken by X-ray diffraction (XRD, Model D/MAX-RB). Raman spectra was recorded by DXR Raman Microscope (Thermo Fisher Scientific) with an excitation length of 532 nm (7 mW) laser. X-ray photoelectron spectroscopy (XPS) analysis were acquired with a twin anode gun, Mg Ka (1253.6 eV) (Microlab 310F Scanning Auger Microprobe, VG SCIENTIFIC LTD). The electric resistivity of as prepared composites was measured on a semiconductor volume resistivity measuring instrument (ST2722, Suzhou Jingge Electronic Co. LTD) ranging from 100 MPa/cm^2 to 180 MPa/cm^2 at 20 MPa/cm^2 intervals. The colorimetric values were evaluated in terms of the Commission Internationale de l'Eclairage (CIE) 1976 $L^*a^*b^*$ colorimetric method by using a Color-Eye automatic differential colorimeter (XTS). Each color in the uniform color space can be denoted by three parameters $L^*a^*b^*$ in rectangular coordinates. L^* presents the lightness axis (0 for black and 100 for white). The parameter a^* means the red-green axis and b^* is blue-yellow axis.

3. Results and discussions

The MT@rGO composite pearlescent pigment was synthesized by a facile three-step route illustrated in Scheme 1. Firstly, the silver white MT pearlescent pigment was prepared by $TiCl_4$ hydrolyzed on the surface of mica flakes, where hydroxyl and carboxyl groups facilitate the binding of TiO_2 nanoparticles. The GO nanosheet was obtained by modified Hummers' method. Because of the strong hydrophilic nature of oxygen functionalities on TiO_2 particles and GO nanosheets, they are easily dispersed in aqueous medium by ultrasonication, separately. Secondly, the homogeneous colloidal solution of GO was dropwise added into MT suspension with vigorous stirring steadily. The available GO nanosheets in the mixture solution could be anchored on to the TiO_2 nanoparticles surfaces, since there are Van der Waals' force and opposite charges attracting [21]. MT@GO composite pearlescent pigment was formed as light precipitate. Finally, the reduction of GO was carried out by mixing MT@GO composite pearlescent pigment and znic powder in acidic solution under stirring. The typical weight of znic powder is ten percent of that of MT@GO composite pearlescent pigment. The color of MT@GO composite pearlescent pigment in suspension solution remained unchanged after mixing znic power, but turned slightly darker accompany with the addition of HCl. The

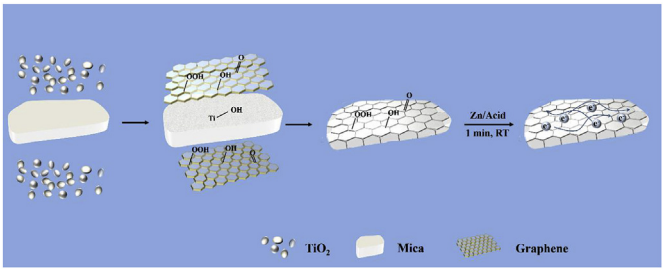

Scheme 1. Scheme illustrating the formation of MT@rGO composite pearlescent pigments.

MT@rGO composite pearlescent pigment was formed within 1 min as color change finished.

3.1. Morphology

The surface and cross-section morphologies of MT@GO-4 and MT@rGO-4 composite pearlescent pigments were characterized by SEM. Fig. 1a and c shows that the whole surface of MT@GO-4 and MT@rGO-4 composite pearlescent pigments have been both homogenously covered by graphene nanosheets. The diameter size of graphene nanosheets is about hundreds nanometer. The shapes of MT@GO-4 and MT@rGO-4 composite pearlescent pigments are flat and irregular flake, whose particle diameter size ranges from 10 to 60 μm as shown in Fig. 1b and d. In Fig. 1e, it can be clearly observed that the dark rGO nanosheets with wavy wrinkles are coating on the surface of MT pigments, as pointed by white line with arrow. It is worth mentioning that MT@GO-4 has to be coated with a thin Au conductive film to minimize charging effects for GO's insulation. On the contrary, the MT@rGO-4 could be directly characterized by SEM without additional treatments, which indicates MT@rGO-4 with conductive performance after reduction from the side.

The pearlescent color effect of MT pigments comes from the light transmittance interference by multiple reflections of inner mica particles and refraction of outer TiO_2 boundary surface [1]. And the optical thickness of TiO_2 layer decided the color effect of MT pigment. Because the optical thickness of nanoparticles is proportional to its geometric thickness, the geometric thickness measurement of TiO_2 layer can reveal the color performance of MT pigment. Fig. 1f describes the cross-section SEM image of the as-prepared MT@rGO-4 composite pearlescent pigment. The outer layer geometric thickness of MT@rGO-4 is 45 ± 4 nm, which suggests that the optical thickness of MT@rGO-4 range from 105 to 124 nm with the TiO_2 refractive index of 2.55. So the MT@rGO-4 composite pearlescent pigment should show silver white pearlescent effect as well as MT pigment (Fig. 7f).

EDS element mapping was used to study the elements distribution of MT@rGO-4 composite pearlescent pigment. As presented in Fig. 2a, it can be found that the surface of MT@rGO-4 is completely covered by graphene nanosheets. Especially, there is some fold graphene combining the two pigments. Since the tight connection of MT@rGO-4 pigments with graphene nanosheets could increase the conductivity of composites directly, it is expected that the MT@rGO-4 should exhibit a good antistatic performance [22]. Fig. 2b–d are EDS element mappings of carbon (C, purple), silicon (Si, blue) and alumina (Al, green), respectively. The black bands, pointed by white line with arrow in Fig. 2b, can be corresponding to the graphene nanosheets with the surface morphology of MT@rGO-4 pigment in Fig. 2a. The Si (Fig. 2c) and Al (Fig. 2d) of mica particle is observed due to the detecting depth of EDS test much more than the thickness of TiO_2 layer (45 ± 4 nm). The EDS spectrum (Fig. 2e) was used to measure the kind and concentration of elements. It shows six peaks corresponding to C, O, Si and Al atom. The C peak further confirms that graphene functional layer has been successfully coated on the surface of MT pigment even after reduction. Most important, the absence of Zn atom in EDS spectrum indicates that Zn particles are entirely removed after reduction.

The surface morphologies of as-prepared MT@rGO-x (x = 1–4) were characterized by SEM to further reveal the relationship between graphene concentration and the color or antistatic performance of composite pearlescent pigments, as displayed in Fig. 3. It is clearly observed that the distribution density of rGO nanosheets on the surface of MT obviously increase with the increasing content of graphene. For example, the surface of MT@rGO-1 is sporadic coated by rGO nanosheets with the diameter size of several hundred nanometers. However, a large number of rGO nanosheets can be both observed on the whole surface of MT@rGO-3 and MT@rGO-4 composite pearlescent pigments. And they connect with each other intensively and continuously in Fig. 3 c and d. Compared with their SEM images, it is worth noting that 3 wt% additive amount of GO nanosheets could be enough to coat on the whole surface of MT pigments. Thus, MT@rGO-3 and MT@rGO-4 may have similar color and antistatic performance, which is verified by the results of later

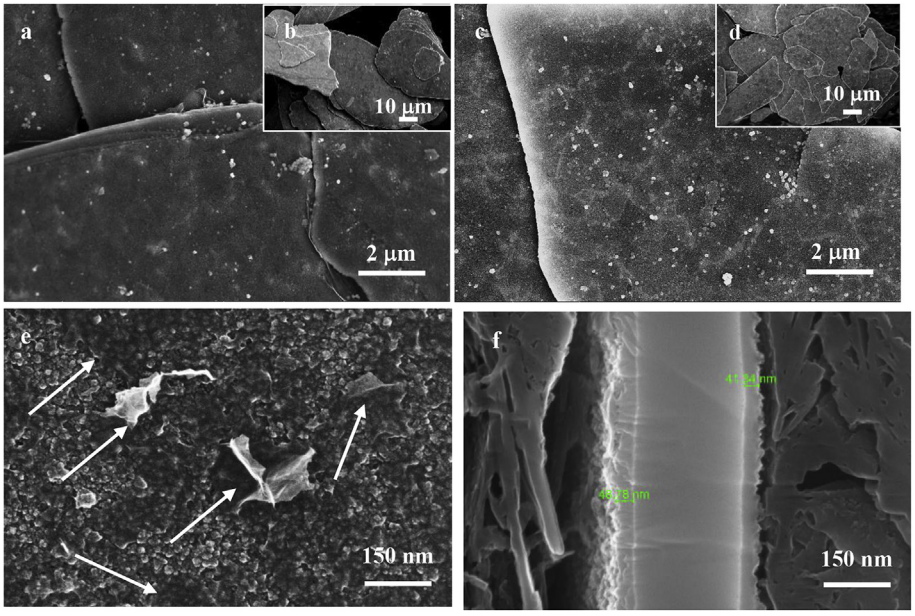

Fig. 1. SEM images of (a) and (b) MT@GO-4 under different magnification; (c)–(e) MT@rGO-4 under different magnification; the rGO nanosheets coated on the surface of MT pigment are pointed by the white line with arrow; (f) cross-section SEM image of MT@rGO-4 composite pearlescent pigment.

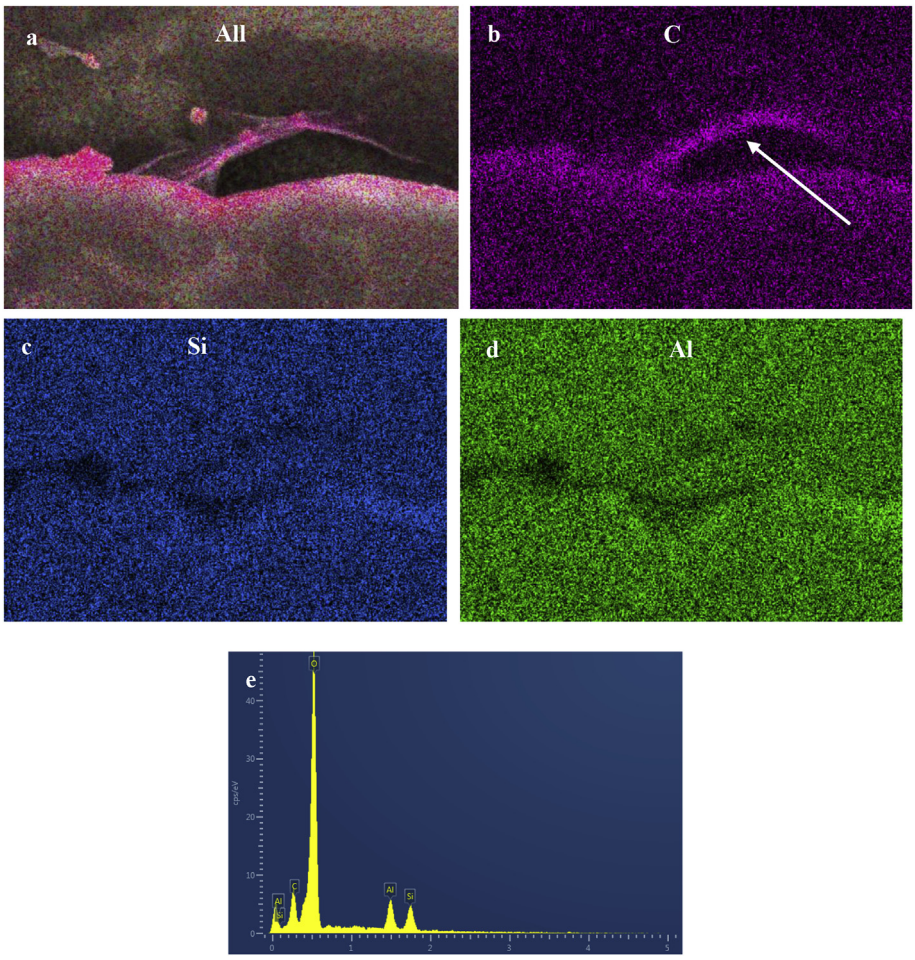

Fig. 2. EDS element mapping profiles of MT@rGO-4 composite pearlescent pigment: element profiles for (a) C-Si-Al overlay; (b) carbon atoms (purple); (c) silicon atoms (blue); (d) alumina atoms (green); (e) the EDS spectrum of MT@rGO-4 composite pearlescent pigment. (For interpretation of the references to colour in this figure legend, the reader is referred to the web version of this article.)

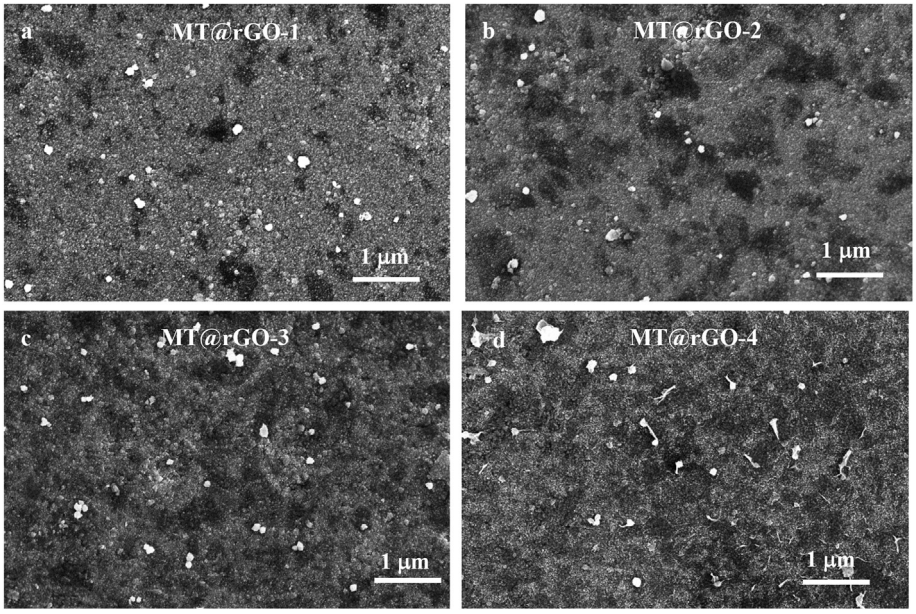

Fig. 3. (a)–(d) surface SEM images of as-prepared MT@rGO-x (x = 1–4) composite pearlescent pigments.

characterization. Based on the above discussion, it can be concluded that the additive amount of graphene oxide have strongly influence on the surface morphology of the obtained composites pearlescent pigments.

3.2. XRD analysis

The phase transformation of mica, TiO_2 and graphite nanoparticles in the series of MT@rGO-x (x = 1–4) composite pearlescent pigments were studied by XRD in Fig. 4, which all pigments exhibit the similar XRD patterns. The four sharp peaks located at 17.67, 26.58, 35.79, 45.25° are attributed to the peaks of potassium mica (JCPDS no. 40–0741) and the peaks appearing at 2θ = 25.39° correspond to (101) plane of anatase TiO_2 (JCPDS no. 21–1272). The patterns mean that mica and anatase TiO_2 has no phase transformation during the preparation procedure. Especially, the similar patterns of MT@rGO-0 and MT pigment in Fig. 4a, indicate that the crystal lattice of MT pigments maintain invariable when znic powder is in direct contact. It implies that the short reduction procedure and room reaction temperature have no influence on the color coordinates of MT pigments. Fig. 4b presents the similar XRD patterns of MT@rGO-x (x = 1–4) composite pearlescent pigments, which means the current concentration of graphene can't affect the phase and component of MT pigments. Nevertheless, the typical diffraction peaks of graphene nanosheets at 2θ angle of 10.9° and 24.57° are not observed for MT@rGO-x (x = 1–4) samples in Fig. 4b [23,24].

3.3. Raman spectra analysis

Raman spectra is a common and non-destructive method to characterize the structural changes of graphene nanosheets before and after reduction. There are two main features used to characterized: the D band at around 1350 cm^{-1} is due to the lattice disorders at the edges and surfaces of small sp^2 clusters, and the G band at around 1600 cm^{-1} comes from the first-order scattering of E_{2g} phonons by sp^2 carbon atoms. Due to the chemical environments of the D and G bands change during reduction procedure, the carbon atoms converse from *sp*2 to *sp*3 hybridization and the conjugated graphene network is reestablished resulting in the increase of I_D/I_G ratio. Compared with that of MT pigment in Fig. 5, the two peaks located at 1350 and 1600 cm^{-1} are characteristic graphite oxide bands in MT@GO-4 and MT@rGO-4 pigments. The intensity ratio of the D and G bands reduction (I_D/I_G) of MT@GO-4 is about 0.9956 and the I_D/I_G ration in the MT@rGO-4 increases to 1.1237 after 1 min reduction of znic powder. It reveals that the MT@rGO-4 composite pearlescent pigment has been successfully

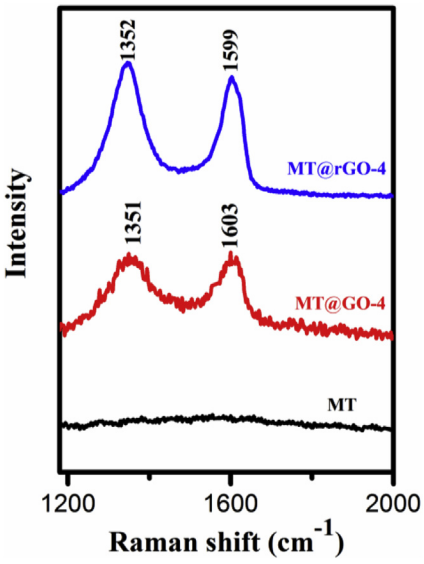

Fig. 5. Raman spectra of MT, MT@GO-4 and MT@rGO-4 composite pearlescent pigments measured at 7 mW laser power and 100 s acquisition time.

achieved by the contact in direct with znic powder. Meanwhile, the increasing interaction between TiO_2 and rGO can be proved by the ca. 3 cm^{-1} blue of G peaks shifts from 1600 cm^{-1} to 1603 cm^{-1} [25].

3.4. XPS analysis

XPS was further used for the qualitative and quantitative detection the surface elemental composition, chemical state and reduction degree of MT@rGO-4 composite pearlescent pigments. The survey spectrum of the MT@GO-4 and MT@rGO-4 composite pearlescent pigments clearly indicates the existence of C, O and Ti (Fig. 6a). As shown in Fig. 6b, the C1s spectra of MT@GO-4 composite pearlescent pigment was deconvoluted into three different peaks centered at 285.0 eV (C-C), 288.9 eV (C=O), and 290.4 eV (C-O) [21]. After reduction, the intensities of the peaks for all oxygen-containing functional groups strongly declined compared with those of MT@GO-4 composite pearlescent pigment (Fig. 6c), attributed to C-C (284.9 eV), C-O (286.6 eV), O-C=O (289.1 eV) and O-C=O (290.8 eV). The degree of GO reduction could be described by the atom ratio of carbon and oxygen taking the ratio of C1s and O1s peak area in XPS spectra. The C/O atomic ratio of MT@GO-4 increased from 0.3655 to 0.8497 that of MT@rGO-4 confirming

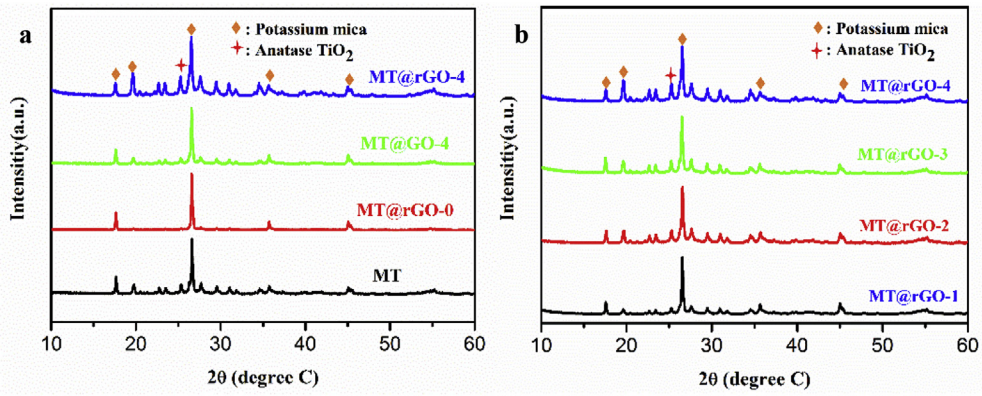

Fig. 4. (a) XRD patterns of MT, MT@GO-4, MT@rGO-0 and MT@rGO-4 composite pearlescent pigments; (b) XRD patterns of MT@rGO-x (x = 1–4) composite pearlescent pigments.

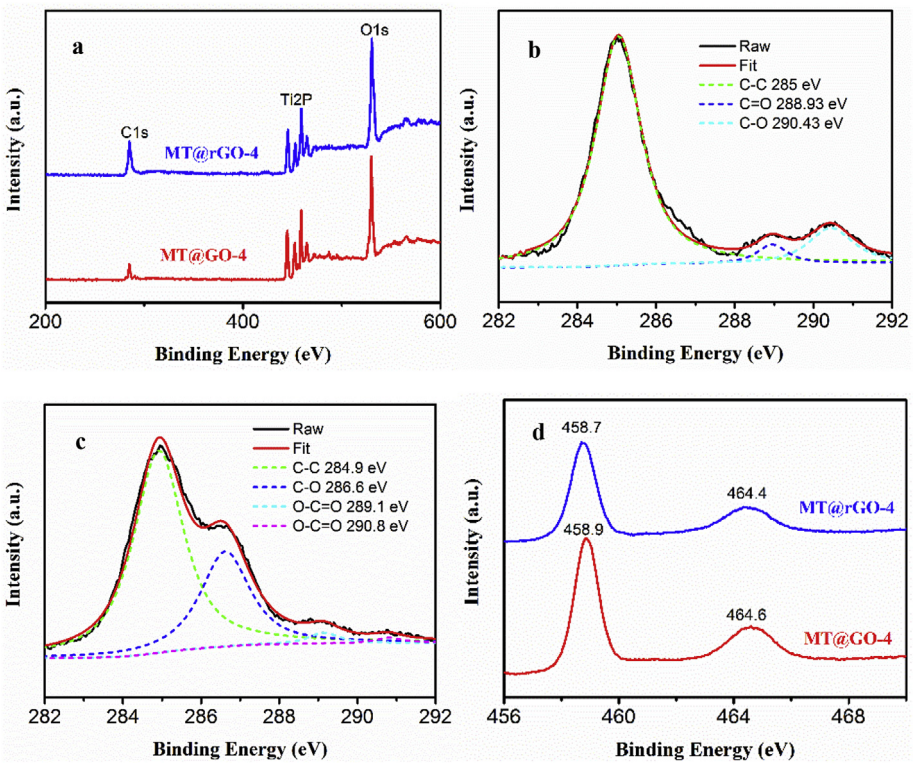

Fig. 6. (a) XPS spectra of MT@GO-4 and MT@rGO-4 composite pearlescent pigments; (b and c) the deconvoluted C1s spectra of MT@GO-4 and MT@rGO-4 composite pearlescent pigments, respectively; (d) Ti 2p XPS core level of MT@GO-4 and MT@rGO-4 composite pearlescent pigments.

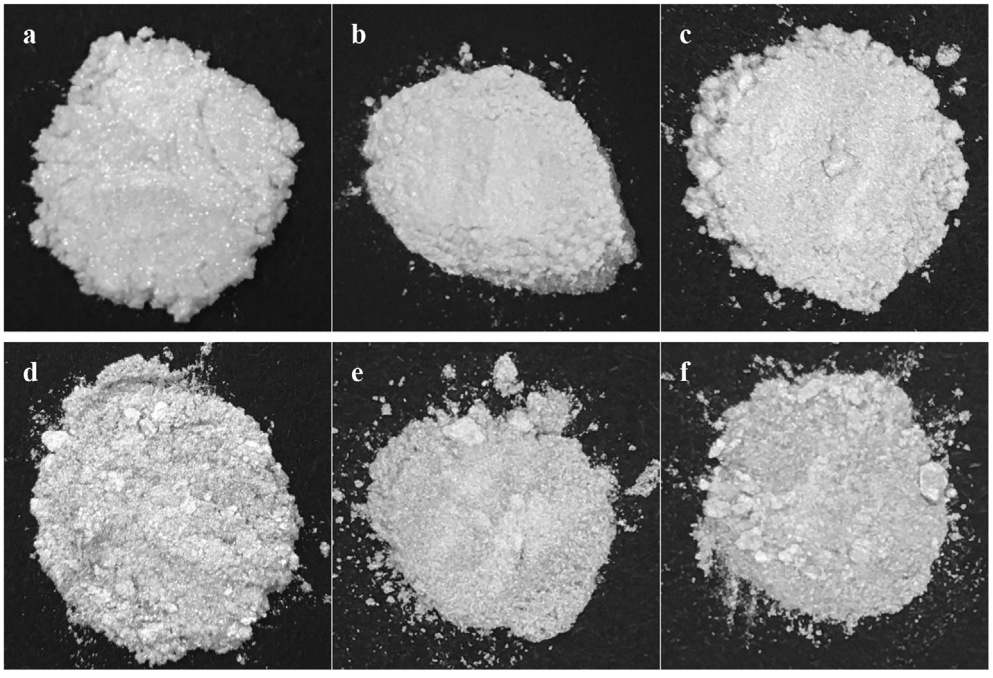

Fig. 7. Photographs of MT (a) and MT@rGO-x (x = 0–4) composite pearlescent pigments treated by znic powder (b) x = 0, (c) x = 1, (d) x = 2, (e) x = 3, (f) x = 4.

the reduction of GO. It agrees with the Raman results.

There are two main peaks in the Ti 2p binding energy region of MT@rGO-4 composite pearlescent pigment in Fig. 6d. The peaks centered at around 458.8 and 464.5 eV are centered at the Ti $2p_{1/2}$ and Ti $2p_{3/2}$ spin-orbital splitting photoelectrons of Ti-O bond in TiO_2. The predominant formation of the Ti^{4+} chemical state in the two composites is proved by the 5.7 eV splitting between Ti $2p_{1/2}$ and Ti $2p_{3/2}$ peaks. Most importantly, the Ti 2p XPS spectral results reveal that the reduction procedure has no effect on the Ti chemical state in TiO_2 nanoparticles of MT pigment. This is one key point for

MT@rGO composite pearlescent pigment to maintain its silver white pearlescent optical effect.

3.5. Optical properties of MT@graphene based composite pearlescent pigments

CIE L*a*b* values of as prepared MT and MT@rGO-x (x = 0–4) pigments samples were used to characterize the color property influence of reduction and summarized in Table 1. All the six pigments display silver white color ($-3.16 < a^* < -2.34$, $-5.79 < b^* < -3.61$). Compared with that of as prepared MT pigment, the L^* (lightness) of MT@rGO-x (x = 0–4) composite pearlescent pigments slightly decrease with the increasing content of rGO. Furthermore, the optical photographs of MT@rGO-x (x = 0–4) composite pearlescent pigments in Fig. 7 show an intuitively color change before and after coating. The reduction procedure results in not obvious green and blue change of MT@rGO composite pearlescent pigments compared with that of raw MT pigment. It is worth mentioning that the color property of MT@rGO-0 could assist to prove the Ti chemical state stable in MT@graphene composite pearlescent pigment under the experimental condition visually as shown in Fig. 7b.

3.6. Volume resistivity measurement

Volume resistivity was measured and used to reveal the antistatic property of MT and MT@rGO-x (x = 1–4) composite pearlescent pigments ranging from 100 MPa/cm^2 to 180 MPa/cm^2 at 20 MPa/cm^2 intervals (Fig. 8). The volume resistivity of MT@rGO-x (x = 1–4) composite pearlescent pigments obviously decreases with the increasing concentration of rGO. And the best electrical property of MT@rGO-3 and MT@rGO-4 composite pearlescent pigments are about 12 kΩ cm, which is over 10^4-fold higher than that of MT composite pearlescent pigment (220 MΩ cm) at the same pressure. The volume resistivity of MT@rGO-x (x = 1–4) composite pearlescent pigments prepared by Ar annealing reduced method and znic powder reduced method at 100 kg/m^2 pressure were listed in Table 2, separately [12]. It can be easily found that the volume resistivity of MT@rGO samples prepared by znic powder reduced method significantly decrease at the same pressure, where those of MT@rGO-1 and MT@rGO-2 prepared decrease over 100 fold. Furthermore, that of MT@rGO-3 markedly decrease 4642 fold. There are two main reasons to explain the good antistatic performance of MT@rGO composite pearlescent pigments in this work. Firstly, the conductivity and contact resistivity of composites can directly be influence by the morphology and continuity of graphene. So, the integrated conductive network of MT@rGO-x (x = 3 and 4) could clearly prove it for the increasing antistatic property as shown in Fig. 3. Secondly, the electrical conductivity of composites is also a critical criteria to evaluate the reduction degree [20]. And we rechecked the volume resistivity of MT@rGO (x = 1–4) composite pearlescent pigments to test their stability after six months

Table 1
Color coordinates, Chroma and Hue angle of MT and MT@rGO-x (x = 0–4) composite pearlescent pigments.

Samples	Color coordinates				
	L^*	a^*	b^*	C^*	h_{ab}/°
MT	64.47	−3.16	−5.79	6.59	241.36
MT@rGO-0	63.93	−2.95	−5.44	6.19	241.51
MT@rGO-1	63.75	−2.70	−4.78	5.49	240.32
MT@rGO-2	62.26	−3.00	−4.74	5.61	237.64
MT@rGO-3	61.95	−2.72	−4.56	5.32	238.95
MT@rGO-4	59.22	−2.34	−3.61	4.30	237.07

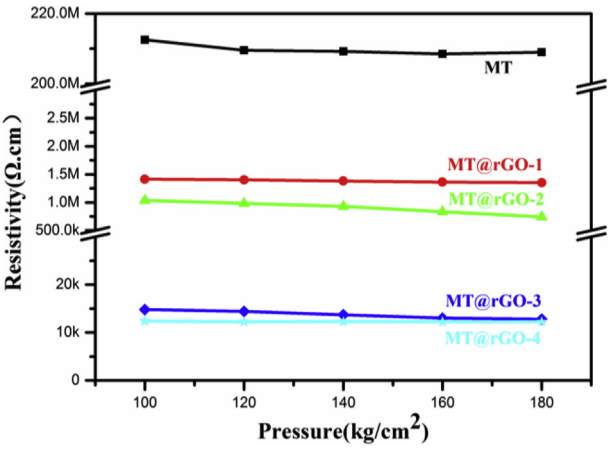

Fig. 8. Volume resistivity of MT@rGO-x (x = 1–4) composite pearlescent pigments measured at the pressure ranging from 100 to 180 kg/cm^2 at 20 MPa/cm^2.

of preparation, which show the antistatic property of these composite pigments is quite stable. The final volume resistivity results prove that znic powder reduction method is quite suitable to prepare high performance MT@rGO composite pearlescent pigments.

3.7. Possible mechanism for the reduction of MT@GO composite pearlescent pigments

The reaction of znic powder and MT@GO-x (x = 1–4) in the acidic solution can be understood in terms of the reduction potentials as following three reactions:

$$Zn \rightarrow Zn^{2+} + 2e^- \quad -0.76\ V$$
$$GO + aH^+ + be^- \rightarrow rGO + cH_2O \quad -0.40\ V$$
$$TiO^{2+} + 2H^+ + e^- \rightarrow Ti^{3+} + H_2O \quad +0.19\ V$$

The standard reduction potential of Zn^{2+} is −0.76 V higher than that of reduction GO potential −0.40 V, which indicate that Zn can effectively reduce GO [20]. On the contrary, the standard reduction potential of Zn^{2+} is lower than that of reduction Ti^{3+} potential +0.19 V. Thus, the chemical state of Ti^{4+} is stable during the reduction procedure, which is consist with the XPS and XRD results. In addition, the coating graphene layer could prevent TiO_2 nanoparticles directly contacting from znic powder [26]. All of these could ensure only GO reduced in MT@GO composite pearlescent pigment so as to save the original silver white color effect of MT pigment.

4. Conclusions

In summary, we have reported a facile and rapid method for preparing MT@graphene based composite pearlescent pigment using znic powder as the reducing agent at room temperature. The optical property of MT pigment can be almost completely saved after be endowed antistatic property. Meanwhile, compared with our previous work, the antistatic performance of as prepared MT@rGO composite pearlescent pigments increase about 100–4600 fold at the same initial concentration of graphene. Most important, MT@rGO composite pearlescent pigment have relative stable optical property and their minimum volume resistivity is about 10^4 Ω cm, which is similar with the traditional MT@ATO composite pearlescent pigment. In addition to, it can be expected to synthesize MT@graphene based composite pearlescent pigments not only reduced by Zn, but also by other metals such as Mg, Al, and Fe as reductant in the future work. This facile preparation method

Table 2
The volume resistivity of MT@rGO-x (x = 1, 2, 3 and 4) composite pearlescent pigments prepared by Ar annealing reduced method and znic powder reduced method at 100 kg/cm^2 pressure.

Sample	Volume resistivity (Ω·cm)		Δ↓
	Ar annealing reduced method	Znic powder reduced method	
MT@rGO-1	1.51×10^8	1.41×10^6	107 fold
MT@rGO-2	1.09×10^8	1.04×10^6	105 fold
MT@rGO-3	6.87×10^7	1.48×10^4	4642 fold
MT@rGO-4	1.43×10^7	1.24×10^4	1153 fold

further prove its superiority of the transparent conductive graphene functional shell for antistatic pearlescent pigments. This process and the high performance of MT@rGO composite pearlescent pigment could be easily adapted for the large-scale application.

Acknowledgements

This work is supported by the National Key Research and Development Program of China (2016YFA0203000) and the National Natural Science Foundation of China (Grant no. 51402340).

References

[1] Maile FJ, Pfaff G, Reynders P. Effect pigments—past, present and future. Prog Org Coatings 2005;54(3):150–63.
[2] Du H, Liu C, Sun J, Chen Q. An investigation of angle-dependent optical properties of multi-layer structure pigments formed by metal-oxide-coated mica. Powder Technol 2008;185(3):291–6.
[3] Pfaff G. Special effect pigments based on silica. Inorg Mater 2003;39(2):170–4.
[4] Santos SF, França SCA, Ogasawara T. Preparation and characterisation of pigments based on mica coated with rare earth oxides. Color Technol 2011;127(5):310–3.
[5] Reynders GPaP. Angle-dependent optical effects deriving from submicron structures of films and pigments. Chem Rev 1999;99:1963–81.
[6] Diebold U. The surface science of titanium dioxide. Surf Sci Rep 2003;48:53–229.
[7] Tan J, Shen L, Fu X, Hou W, Chen X. Preparation and conductive mechanism of mica titania conductive pigment. Dyes Pigments 2004;62(2):107–14.
[8] Topuz BB, Gündüz G, Mavis B, Çolak Ü. The effect of tin dioxide (SnO2) on the anatase-rutile phase transformation of titania (TiO2) in mica-titania pigments and their use in paint. Dyes Pigments 2011;90(2):123–8.
[9] Kim H, Piqué A. Transparent conducting Sb-doped SnO2 thin films grown by pulsed-laser deposition. Appl Phys Lett 2004;84(2):218–20.
[10] Wu J-M. Characterizing and comparing the cathodoluminesence and field emission properties of Sb doped SnO2 and SnO2 nanowires. Thin Solid Films 2008;517(3):1289–93.
[11] Tan J, Shen L, Fu X, Hou W, Chen X. Preparation of nanometer-sized (1−x) SnO2·xSb2O3 conductive pigment powders and the hydrolysis behavior of urea. Dyes Pigments 2004;61(1):31–8.
[12] Wang Y, Liu M, Liu Y, Luo J, Lu X, Sun J. A novel mica-titania@graphene core-shell structured antistatic composite pearlescent pigment. Dyes Pigments 2017;136:197–204.
[13] Lee MS, Lee K, Kim SY, Lee H, Park J, Choi KH, et al. High-performance, transparent, and stretchable electrodes using graphene-metal nanowire hybrid structures. Nano Lett 2013;13(6):2814–21.
[14] Chua CK, Pumera M. Chemical reduction of graphene oxide: a synthetic chemistry viewpoint. Chem Soc Rev 2014;43(1):291–312.
[15] Wang F, Zhang K. Reduced graphene oxide–TiO2 nanocomposite with high photocatalystic activity for the degradation of rhodamine B. J Mol Catal A Chem 2011;345(1–2):101–7.
[16] Kim NH, Khanra P, Kuila T, Jung D, Lee JH. Efficient reduction of graphene oxide using Tin-powder and its electrochemical performances for use as an energy storage electrode material. J Mater Chem A 2013;1(37):11320.
[17] Barman BK, Mahanandia P, Nanda KK. Instantaneous reduction of graphene oxide at room temperature. RSC Adv 2013;3(31):12621.
[18] Compton OC, Nguyen ST. Graphene oxide, highly reduced graphene oxide, and graphene: versatile building blocks for carbon-based materials. Small 2010;6(6):711–23.
[19] Mei X, Zheng H, Ouyang J. Ultrafast reduction of graphene oxide with Zn powder in neutral and alkaline solutions at room temperature promoted by the formation of metal complexes. J Mater Chem 2012;22(18):9109.
[20] Mei X, Ouyang J. Ultrasonication-assisted ultrafast reduction of graphene oxide by zinc powder at room temperature. Carbon 2011;49(15):5389–97.
[21] Perera SD, Mariano RG, Vu K, Nour N, Seitz O, Chabal Y, et al. Hydrothermal synthesis of graphene-TiO2Nanotube composites with enhanced photocatalytic activity. ACS Catal 2012;2(6):949–56.
[22] Zhang LL, Zhao X, Stoller MD, Zhu Y, Ji H, Murali S, et al. Highly conductive and porous activated reduced graphene oxide films for high-power supercapacitors. Nano Lett 2012;12(4):1806–12.
[23] Štengl V, Popelková D, Vláčil P. TiO2–Graphene nanocomposite as high performace photocatalysts. J Phys Chem C 2011;115(51):25209–18.
[24] Zhang H, Lv X, Li Y, Wang Y, Li J. P25-Graphene composite as a high performance photocatalyst. ACS Nano 2010;4:380–6.
[25] Liu S, Wang R, Liu M, Luo J, Jin X, Sun J, et al. Fe2O3@SnO2 nanoparticle decorated graphene flexible films as high-performance anode materials for lithium-ion batteries. J Mater Chem A 2014;2(13):4598.
[26] Yu Z, Di H, Ma Y, He Y, Liang L, Lv L, et al. Preparation of graphene oxide modified by titanium dioxide to enhance the anti-corrosion performance of epoxy coatings. Surf Coatings Technol 2015;276:471–8.